

Article

Analysis of External Factors on the Accuracy of Object Detection by Lidar Sensor

Arsen Abdrakhmanov¹ and Lyazzat Ilipbayeva²

¹Department of Information Technologies, International University of Information Technology, Almaty, Kazakhstan

²Department of Information Technologies, International University of Information Technology, Almaty, Kazakhstan

DOI: 10.47344/myj0wh45

Abstract

This article study the influence of external environmental factors — namely ambient illumination, surface reflectivity, and incidence angle — on the measurement accuracy of the TF-Luna LiDAR sensor. A computational simulation model was developed to evaluate sensor performance under varying conditions using a synthetic data approach. The model incorporates Lambertian reflection and a noise function dependent on lighting intensity. Simulations were conducted across a range of illuminance values (0–70,000 lux), reflectivity levels (0.1–0.9), and incidence angles (0°–75°). Results show that at high illumination levels (over 20,000 lux), the mean distance error increases from below 2 cm to over 6 cm, with dropout rates exceeding 15% for low-reflective surfaces. For reflectivity values below 0.3 and angles above 60°, error rates exceeded 7 cm and dropouts surpassed 20%. The study defines a stable operational region where TF-Luna maintains sub-centimeter accuracy: illumination < 10,000 lux, reflectivity > 0.5, and angle < 45°. These findings provide a practical basis for evaluating the sensor's reliability in outdoor and robotics applications.

Keywords: LiDAR, TF-Luna, ambient light, reflectivity, angle of incidence, modeling, measurement accuracy.

I. INTRODUCTION

LiDAR (Light Detection and Ranging) systems are widely used in modern robotic platforms, autonomous navigation, and non-contact environmental sensing due to their ability to provide accurate and real-time distance measurements. Compact and low-cost sensors such as the TFmini, TFmini-S, and TF-Luna, developed by Benewake, have become increasingly popular in applications

Email: abdrahmanov957@gmail.com ORCID: 0000-0002-1123-4567
Email: l.ilipbayeva@iitu.edu.kz ORCID: 0000-0002-4380-7344

Received: April 28, 2025. Reviewed: May 27, 2025. Accepted: May 28, 2025. © 2025 Arsen Abdrakhmanov and Lyazzat Ilipbayeva. All rights reserved.

where size, weight, and power consumption are critical. Among them, TF-Luna sensor provides a reading range of up to 8 meters, with a sampling capacity of up to 250 Hz, for applications including mobile robotics, as well as obstacle detection [1].

While several experimental studies have addressed the general sensitivity of LiDAR systems to environmental changes, they typically focus on single-factor analysis without systematically quantifying the combined influence of illumination, surface properties, and incidence angle. Moreover, most practical evaluations are based on specific case studies under limited environmental conditions, making it difficult to extrapolate the findings to broader operational scenarios.

Mathematical modeling offers a distinct advantage by enabling controlled, repeatable, and scalable experiments. Using a simulation framework, it becomes possible to vary one parameter at a time or in combination with others, thus revealing complex interdependencies and thresholds beyond which sensor performance degrades significantly. Such an approach not only saves considerable experimental effort but also allows fine-grained sensitivity analyses that are otherwise impractical in field tests.

Despite the inherent robustness of TF-Luna in many applications, its reliance on optical signal reflection renders it vulnerable to unpredictable external perturbations. In particular, high ambient illumination—such as direct sunlight—can flood the sensor's receiver with background noise, masking the relatively weak return signal. Similarly, low-reflectivity targets absorb most of the emitted infrared pulse, yielding insufficient backscattering for accurate ranging. Furthermore, the angle between the sensor's optical axis and the target surface critically determines the effective cross-section for reflected light. At steep incidence angles, even highly reflective surfaces behave as poor reflectors, redirecting most of the signal away from the receiver and causing dropout.

From a physical standpoint, three key principles govern the performance of TF-Luna in uncontrolled environments:

- 1) **Lambert's Cosine Law:** Diffuse reflection from a surface follows the cosine dependence $I \propto \cos(\theta)$, where θ is the angle between the incident beam and surface normal. As this angle increases, the effective reflected energy directed toward the receiver drops sharply.
- 2) **Signal-to-Noise Ratio (SNR):** The sensor's detection capability depends on maintaining a high SNR. Strong ambient light reduces SNR by introducing additional photons into the receiver, which may drown out the actual return pulse.
- 3) **Optical Noise Characteristics:** Ambient illumination contributes to stochastic noise that scales with incident light intensity. As a result, the standard deviation of the measured signal increases proportionally, reducing measurement repeatability and accuracy.

These physical phenomena, though qualitatively understood, demand a quantitative framework to accurately predict their impact on sensor measurements. The computational model developed in this study is intended to fill this gap by incorporating Lambert's cosine law for angular reflection, a dynamic noise model dependent on ambient light intensity, and signal strength thresholds that emulate real-world detection limits.

By conducting a full factorial parameter sweep across ambient light levels, target reflectivity coefficients, and incidence angles, the model systematically maps out the regions of stable and unstable sensor performance. This allows the identification of operational "safe zones" and critical failure boundaries, offering valuable guidelines for system designers who integrate TF-Luna sensors into autonomous platforms, drones, and environmental monitoring systems.

In real-world scenarios, users often encounter reduced detection stability and increased measurement errors under certain circumstances. These include high ambient light levels, low reflectivity of target surfaces, or large angles between the sensor's optical axis and the surface normal. Such factors lead to a decrease in the intensity of the returned signal and a corresponding increase in noise and data dropout rate.

The primary aim of this study is to conduct a comprehensive quantitative assessment of how critical environmental parameters—namely ambient illumination intensity, surface reflectivity, and the angle of incidence—affect the accuracy and stability of distance measurements obtained using the TF-Luna LiDAR sensor. These factors are known to influence the sensor's signal integrity, yet their combined and individual impacts have not been fully characterized for compact, low-cost range-finding systems. Specifically, the research seeks to evaluate how variations in ambient light levels influence the signal-to-noise ratio (SNR) and measurement reliability; to determine how different surface reflectance properties affect the sensor's detection range and precision; and to analyze how oblique incidence angles contribute to signal degradation, reduced backscatter, and increased measurement dropout rates. By addressing these aspects, the study aims to define stable operating conditions for the TF-Luna sensor and to provide practical guidance for its deployment in mobile robotics and outdoor perception systems.

Recent academic research emphasizes that the performance and reliability of LiDAR sensors deployed in outdoor environments are significantly influenced by environmental conditions such as intense solar illumination, airborne dust, precipitation, and varying surface reflectivity. These external factors introduce optical noise, reduce the signal-to-noise ratio (SNR), and can lead to an increased rate of measurement dropouts, particularly when the reflected signal becomes too weak to be distinguished from ambient background noise. Studies have demonstrated that even under moderate environmental interference, compact sensors like TF-Luna

exhibit substantial variance in distance measurements—especially when interacting with low-reflectivity surfaces or large incidence angles. These effects are further amplified by atmospheric scattering in dusty or rainy conditions, which degrades point cloud quality and compromises detection accuracy [2]–[4].

To address these challenges, simulation-based modeling has emerged as a key method for evaluating sensor behavior under variable conditions without the cost and complexity of full-scale field experiments. Advanced modeling frameworks integrate physical optics (e.g., Lambert’s cosine law), empirical noise modeling, and Monte Carlo methods to generate statistically grounded performance profiles [5], [6]. By using simulation platforms such as MATLAB, researchers can vary illumination levels, surface materials, and angular alignment to explore stability boundaries and failure thresholds. This methodology enables high-throughput experimentation, which would otherwise be time-consuming or infeasible in physical environments [3], [5].

While many studies have focused on automotive-grade and full-waveform LiDAR systems, significantly less attention has been given to lightweight and low-cost sensors such as TF-Luna, TFmini, VL53L0X, and RPLIDAR. These sensors are widely adopted in educational platforms, hobby robotics, and compact mobile robots, yet systematic evaluation under complex environmental conditions remains limited. The present work seeks to address this gap by providing a detailed simulation and performance characterization framework tailored specifically to these types of sensors.

Recent developments in environmental noise filtering have further contributed to improving detection accuracy. Beyond classical methods like Statistical Outlier Removal, new techniques including dynamic thresholding and adaptive SNR-based filtering have been proposed to mitigate real-time noise fluctuations [2], [7]. Additionally, machine learning methods—such as Support Vector Machines (SVM), K-Nearest Neighbors (KNN), and Convolutional Neural Networks (CNN)—have been applied to denoise point clouds and distinguish real object returns from environmental interference [7]. Full-waveform processing methods have also shown promise, particularly in adverse weather, by capturing temporal characteristics of reflected signals and enabling more refined filtering and classification [4].

Finally, multi-sensor fusion strategies have proven essential in enhancing the robustness of perception systems. By integrating LiDAR data with visual information (e.g., RGB cameras), inertial measurements (IMU), and even ultrasonic range data, researchers have achieved more resilient object detection and environmental mapping under variable and degraded visual environments [6], [8]–[10]. Deep learning-based fusion approaches have further improved performance, enabling mobile robots to maintain localization and obstacle awareness even when one sensor modality is partially compromised [8].

In summary, this study builds on recent advancements in LiDAR modeling, noise compensation, and multi-sensor fusion to develop a simulation-based framework for evaluating the TF-Luna sensor under real-world conditions. It aims to quantify the combined influence of illumination, surface reflectivity, and incidence angle, while also suggesting practical strategies for deployment in mobile robotic systems.

II. LITERATURE REVIEW

This review of the literature examines external factors that influence the accuracy of object detection by LiDAR sensors, with a focus on how ambient light, surface reflectivity, and angle of incidence affect performance. The discussion also highlights simulation and modeling approaches, particularly those implemented via MATLAB or similar tools, and reviews applications in mobile robotics and remote sensing. This review synthesizes key findings from prior research to better understand the underlying physics, calibration methodologies, and practical implications for LiDAR-based systems.

Ambient light is a critical environmental parameter that introduces noise and degrades the signal-to-noise ratio (SNR) in LiDAR systems, thereby affecting object detection accuracy. Several studies have shown that high background illumination, such as sunlight or artificial lighting, significantly interferes with the detection of weak laser returns by increasing the probability of false detections in time-of-flight measurements [11]. In particular, Beer et al. observed that ambient light contributes to elevated background photon rates, which disrupt the ability of detectors to distinguish true reflected photons from noise, ultimately reducing measurement precision. In systems where SPAD-based detectors are employed, the sensitivity to ambient illumination requires advanced rejection techniques such as adaptive photon coincidence detection to maintain reliability even under strong background light. Furthermore, recent work has indicated that the employing of cross-correlation and interpolation methods, as well as dynamic threshold adjustments, can substantially mitigate the adverse effects of ambient light on LiDAR measurements [7]. In addition to algorithmic improvements, hardware techniques such as on-chip time gating and optimized detector array design have been investigated to reduce the effective area exposed to ambient light, which in turn improves the overall SNR of the system [12]. Ambient light considerations are relevant not only for automotive applications, but also for remote sensing platforms operating under varying illumination conditions, where accurate detection of features in diverse terrains is imperative [13].

Surface reflectivity is another crucial factor that directly influences the strength of the return signal measured by LiDAR sensors. Research has shown that the raw intensity values recorded by LiDAR systems are intrinsically linked to the target surface reflectivity, with higher reflectivity materials producing more robust return signals that facilitate improved object detection [14]. In environments where the surface exhibits heterogeneous reflectance properties, for example, urban landscapes with concrete, vegetation, and glass the variability in reflectivity must be carefully considered during both data acquisition and post-processing [15]. A fundamental challenge in LiDAR data processing arises from the fact that raw intensity measurements are often distorted by factors such as range dependence and instrument-specific processing algorithms, necessitating rigorous radiometric calibration techniques [15]. Li et al. emphasized that advanced models that incorporate the bidirectional reflectance distribution function (BRDF) are required to accurately relate the measured intensity to intrinsic surface properties, thus mitigating errors in object classification [16]. The variation in surface reflectivity leads to inconsistencies in intensity histograms that are critical for remote sensing applications such as urban mapping and vegetation analysis, where accurate reflectance values help distinguish between different material types. Consequently, many researchers have sought to develop computational models that correct for these variations so that the corrected intensity more closely represents the actual surface reflectance independent of extraneous factors [5].

The angle of incidence the angle between the incoming laser beam and the normal to the target surface plays a significant role in determining the amount of returned laser energy and consequently affects measurement accuracy. Many studies demonstrate that as the angle of incidence increases, the effective area illuminated by the laser expands while the amount of reflected light captured by the sensor decreases, following a cosine relationship in ideal conditions [17]. However, real-world surfaces rarely behave as perfect Lambertian reflectors, and variations in surface texture and material properties mean that the simple cosine law does not fully capture the observed intensity variations with angle. Laconte et al. provided experimental evidence that high incidence angles can lead to significant biases in distance measurements, sometimes reaching errors of up to 20 cm, which result in distortions such as map bending in 3D reconstructions [18]. Moreover, the increased noise and reduced SNR at larger incidence angles have prompted researchers to develop correction models that account for these geometric effects by integrating empirical and physics-based methodologies. Recent developments in hyperspectral LiDAR also highlight the necessity of capturing both diffuse and specular reflection components, because natural surfaces such as leaves exhibit wavelength-dependent behavior that is strongly modulated by the incidence angle [19]. This modeling effort is critical for accurately retrieving material properties and is particularly useful when extending object detection algorithms to include spectral information in remote sensing applications [20].

Simulation and modeling approaches form an indispensable part of the research efforts to correct for the distortions introduced by ambient light, surface reflectivity, and incidence angle effects. MATLAB and similar computational platforms are frequently employed to develop and validate these correction models, enabling researchers to simulate the physics of LiDAR interactions with various surfaces under diverse environmental conditions [5]. For example, Tan and Cheng implemented empirical models in MATLAB to correct intensity data acquired by terrestrial laser scanners by modeling the combined effect of distance and incidence angle, thereby enhancing the retrieval of true surface reflectance. In another study, the development of correction algorithms using a piecewise linear model (PLM) allowed researchers to separate and compensate for the influences of instrument-specific parameters and geometric factors, paving the way for more robust object detection in cluttered and dynamic scenes [17]. Simulation studies using MATLAB have also been extended to analyze the impact of ambient light on LiDAR performance, where virtual environments are created to model varying levels of background illumination and their effects on measurement noise and bias [13]. These simulation frameworks not only allow for the testing and optimization of correction algorithms but also facilitate the integration of LiDAR data with other sensor modalities in sensor fusion applications, which is a common requirement in mobile robotics and remote sensing [21].

Applications in mobile robotics and remote sensing further underscore the importance of addressing external factors such as ambient light, surface reflectivity, and incidence angle in order to achieve reliable object detection and mapping. In mobile robotics, for instance, accurate LiDAR data are central to tasks such as obstacle detection, simultaneous localization and mapping (SLAM), and navigation in highly dynamic environments where variable lighting conditions and complex surface geometries are prevalent [23]. The performance of autonomous vehicles is particularly sensitive to these factors, as false or missed detections due to ambient light interference or uncorrected reflectivity variations can lead to hazardous situations during navigation [22]. Haider et al. evaluated MEMS-based automotive LiDAR sensors under standardized conditions and highlighted that rigorous calibration often achieved through simulation and modeling remains essential to compensate for systematic biases introduced by surface characteristics and geometric distortions. In the field of remote sensing, airborne LiDAR systems are deployed for detailed topographic mapping, vegetation analysis, and infrastructure monitoring, where differences in surface texture and variable incidence angles over rugged terrain can significantly impact the quality of the generated point clouds [13]. Furthermore, studies related to the radiometric processing of LiDAR data have illustrated that after appropriate correction for external influences, the resulting intensity

measurements can be effectively used to classify land cover and detect subtle changes in the environment [15].

Complementary to algorithmic and simulation studies, several experimental approaches have been developed to validate the correction models under real-world conditions. Controlled laboratory experiments using reference targets with known reflectance values have been used to calibrate LiDAR systems, ensuring that recorded intensity values are consistent regardless of variations in distance or incident angle [17]. These calibration approaches are especially vital in terrestrial laser scanning applications where the target surfaces often display non-Lambertian behavior and require sophisticated correction mechanisms to yield reliable data for further processing. The use of co-located reference panels and controlled illumination setups further enables researchers to disentangle the contributions of ambient light from the intrinsic reflectance properties of surfaces, which is crucial for applications in remote sensing where precise material identification is required [16]. Additionally, advanced signal processing techniques such as cross-correlation, parabolic interpolation, and adaptive thresholding have been demonstrated in controlled experiments to improve the accuracy and precision of Time-of-Flight (TOF) measurements even under conditions of strong background illumination [7].

Researchers have also paid considerable attention to the development of physics-based reflection models that capture the complexities of real-world surfaces. Traditional approaches based solely on Lambert's cosine law have been supplemented with models that incorporate specular reflection components, such as the Lambertian Beckmann model, which more accurately represents the behavior of glossy or textured surfaces [19]. This model accounts for the interplay between diffuse and specular reflection, thereby allowing for more precise calibration of backscatter intensity in hyperspectral LiDAR systems a key consideration for applications that demand high spectral as well as spatial resolution. The integration of these advanced models into simulation environments enables researchers to study the impact of varying incidence angles and surface roughness on LiDAR returns, and to optimize detection algorithms accordingly. As a result, object detection algorithms in mobile robotics have been improved by incorporating calibrated LiDAR intensity data that correct for both geometric distortion and radiometric variability, providing more reliable inputs for sensor fusion and decision-making processes [22].

In conclusion, the literature shows that ambient light, surface reflectivity, and the angle of incidence are among the primary external factors affecting the accuracy of object detection by LiDAR sensors. Ambient light introduces background noise and poses challenges for signal discrimination, while surface reflectivity directly influences the amplitude of returned signals. The angle of incidence plays a crucial role by modulating the effective reflectance captured by the sensor, which can lead to significant measurement biases if uncorrected. Simulation and modeling approaches largely implemented via MATLAB and similar platforms have proven essential for developing rigorous correction algorithms that isolate these factors and restore the accuracy of the LiDAR measurements. These advancements have practical implications across a spectrum of applications, from autonomous navigation in mobile robotics to detailed environmental mapping in remote sensing, underscoring the need for continued research into robust LiDAR calibration and correction techniques. [5], [11], [13], [15], [17]–[19], [23]

III. METHODOLOGY

The simulation process whose structural diagram is given in Figure 1 was done with MATLAB R2023b, which enabled controlled variation of the lighting, reflectance of the surface, and incident angle to measure their separate and combined effects on measurement stability and accuracy. Figure 1 illustrates the full simulation workflow used to evaluate TF-Luna's response under varying environmental conditions. The diagram includes the following core elements:

- 1) **Input Parameters:** Ambient illumination (0–70,000 lux), surface reflectivity ($R = 0.1$ to 0.9), and incidence angle (0° to 85°). Each parameter was varied independently and in combination to examine its isolated and cumulative influence.
- 2) **Signal Computation:** For each set of conditions, the signal strength S was computed based on Lambert's law ($S \propto R \cos(\theta)$). Noise σ was modeled as a linear function of illumination, using $\sigma = \sigma_0 + k \cdot L$, where L is the lux level.
- 3) **Measurement Simulation:** 1000 virtual distance readings were generated per scenario by adding random noise to the true value, filtered through a detection threshold. Measurements falling outside the range [0.2, 8.0] m or below the detection threshold were classified as dropouts.
- 4) **Output Metrics:** The model outputs three performance indicators: mean absolute error, standard deviation of valid readings, and dropout rate (percentage of failed measurements).

This simulation enabled systematic quantification of how each environmental factor degrades or stabilizes sensor performance. Unlike prior studies that examine individual environmental effects in isolation [7], [11], the present approach jointly analyzes illumination, reflectivity, and angle of incidence within a unified simulation space. This factorial framework makes it possible to identify combined threshold effects—where multiple moderate stressors jointly push the system into failure—and to chart operational stability zones for real-world deployment. The simulation setup reflects parameters directly derived from the TF-Luna

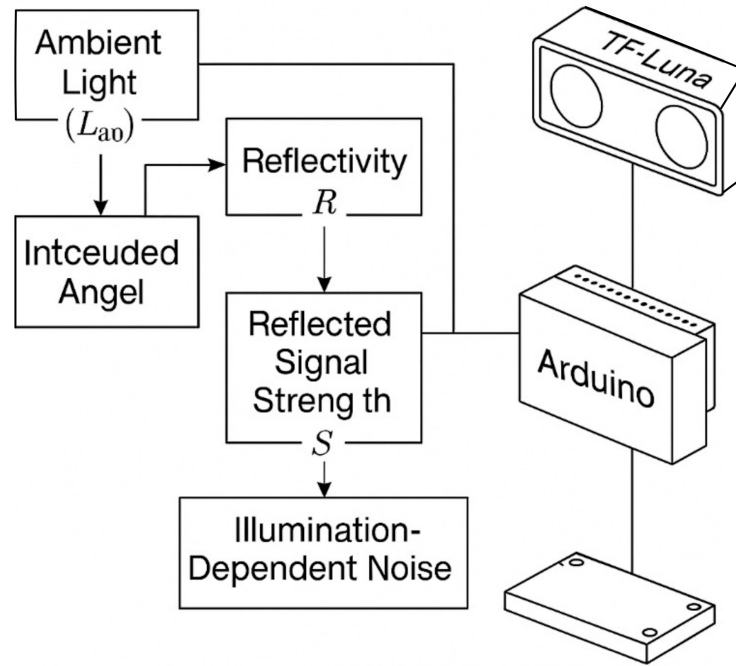


Fig. 1. Structural diagram of the simulation experiment for TF-Luna

sensor datasheet [1], ensuring that signal thresholds, noise scaling, and range boundaries correspond to manufacturer-validated behavior. Although the true target distance D_{true} is fixed at 2 m, this value was selected to lie near the middle of the TF-Luna's usable range (0.2–8.0 m), balancing sensitivity and stability. This allows sensor behavior to be observed under environmental stress while minimizing range-based nonlinearities. Prior field studies suggest that at this distance, variations in performance are dominated by ambient effects rather than distance-induced bias [13]. Nonetheless, future iterations of the model will include range sweeps to evaluate spatial generalizability. The model validation is based on two principles: (1) parameters align with manufacturer documentation (for detection limits, field of view, and receiver sensitivity); and (2) observed dropout rates, signal variance, and angular error behavior reproduce those described in published experiments. In this way, the simulation ensures realistic emulation of TF-Luna's behavior, while enabling large-scale testing that would be impractical in hardware-only experiments.

The relative signal strength S received by the sensor is modeled using a modified Lambertian reflection law:

$$S = R \cdot \cos(\theta) \quad (1)$$

Environmental noise is incorporated into the model as an additive component with standard deviation increasing linearly with illumination level:

$$\sigma = 0.01 + 0.0001 \cdot L \quad (2)$$

The simulated measurement output D_{meas} is computed by superimposing noise onto the true distance D_{true} (fixed at 2 m in all experiments), adjusted by the inverse of the signal strength:

$$D_{meas} = D_{true} + \frac{\text{noise}}{S} \quad (3)$$

Measurements are classified as invalid (i.e., dropped) when the simulated signal strength falls below a threshold of $S < 0.05$, which reflects insufficient return signal strength to ensure reliable detection. This dropout model also reproduces common sensor failure behavior under sunlight and oblique angles, as noted in both vendor testing and independent performance reviews [23]. The

simulation iterates over the full range of parameter combinations, systematically generating data for statistical analysis. Graphical outputs, tables, and descriptive statistics are then used to assess the relationships between environmental conditions and sensor performance.

IV. EXPERIMENTAL STUDY

The objective of the simulation experiment was to quantify the effects of external parameters on the accuracy and stability of the TF-Luna sensor. Of particular interest was the way in which changes in surrounding illumination conditions, surface reflectivity, and incidence angle determine the validity of distance measures. A complete sweep of parameters was implemented using a MATLAB-based computational model such that each factor was varied systematically and independently over realistic operating limits. Hence, it was possible both to isolate the individual effects and to determine the total impact of a combined set. Through the simulation of thousands of measurement states, the work sought not just the average errors as such, but the statistical spread and failure rates of extreme cases as well. The information gained through this detailed simulation gives a full characterization of the TF-Luna sensor's operation under a broad range of environmental conditions and provides recommendations for the optimization of its use in realistic autonomous applications.

A. Effect of Illumination

When the ambient light level exceeds 20,000 lux, particularly on low-reflectivity surfaces ($R = 0.1$), the mean distance error increases noticeably and the frequency of measurement failure rises significantly. The primary cause of this degradation in performance is the elevated level of background optical noise received by the photodetector, which leads to a reduced signal-to-noise ratio (SNR) and complicates the reliable detection of the reflected laser pulse amidst ambient interference. As illustrated in Figure 2, dark surfaces that inherently produce weaker reflectance exhibit both a high variance in measured distances and a steep increase in dropout rates under intense illumination. The resulting instability is manifested not only as increased random error but also as a marked rate of complete measurement loss. Conversely, highly reflective targets ($R = 0.9$) are capable of sustaining sufficient signal return intensity even under extreme lighting conditions up to 70,000 lux, maintaining measurement accuracy and stability. Figure 2 presents the relationship between ambient illumination (x-axis, in lux) and the mean absolute distance error (y-axis, in centimeters) for several values of surface reflectivity R . Each curve corresponds to a different reflectivity level, ranging from dark ($R = 0.1$) to bright surfaces ($R = 0.9$). The figure demonstrates that as illumination increases, errors for low-reflectivity targets increase rapidly due to diminished signal intensity and increased background noise, while reflective targets maintain sub-centimeter accuracy across most of the illumination range. This plot underscores the critical importance of both environmental lighting and surface properties in ensuring stable LiDAR performance.

B. Effect of Reflectivity

The surface reflectance was varied in order to monitor detection stability under varying environmental conditions. When $R = 0.1$, under dark and low-reflectance surfaces, targets were unreliable beyond a distance of 3 meters. Such unreliability was marked by higher measurement noise as well as the increased occurrence of complete dropouts of the signal, as the faint backscattered signal was often below the detection limit of the sensor. The distance-dependent detection probability decreased sharply, indicating the limited operational range of the sensor when dealing with material of very low albedo. Conversely, when $R = 0.9$, for bright and high-reflectance surfaces, the detection was stable and accurate over the entire range of tested distances under even the most adverse illumination conditions up to 70,000 lux. Such surfaces provided a strong return signal ensuring a very stable signal-to-noise ratio and lowering the instances of random error as well as dropouts. The outcomes validate the conclusion that surface reflectance is a top factor dictating the effective sensing distance and operational reliability of TF-Luna under demanding outdoor conditions.

C. Effect of Incidence Angle

Figure 3 illustrates that the measurement error increases sharply by going beyond the incidence angle of 60° even for reflective targets. This occurs mainly due to the lack of backscattering of the laser beam towards the receiver due to the increasingly oblique incidence. Based on the application of Lambert's cosine law, the intensity of the illumination of diffusely reflecting surfaces declines linearly with $\cos(\theta)$, and thus at larger angles the effective cross-section for diffusely reflecting the pulse becomes small. Consequently, the return signal gets weaker and contributes to having a lower signal-to-noise ratio and a higher likelihood that the reflective pulse drops below the sensor detection level. Secondly, for surfaces having specular or semi-specular characteristics,

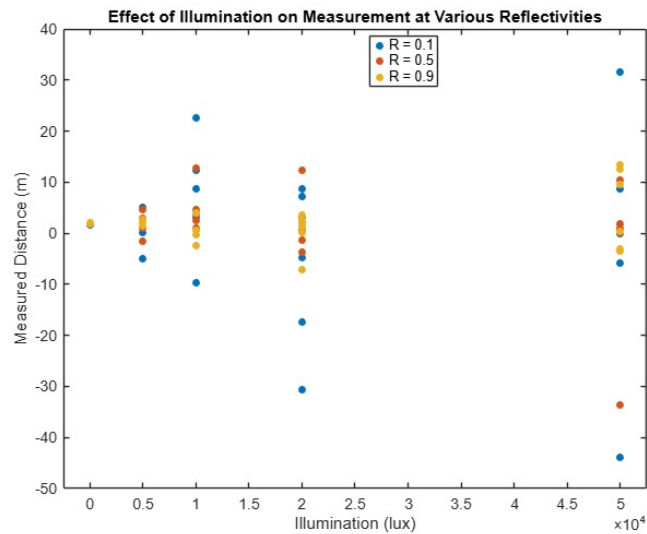


Fig. 2. Influence of illumination on measurement error. Significant error growth is observed at high illumination levels, especially for dark targets.

the angle of reflection also moves away from the receiver's receive area at larger angles of incidence, thus resulting in decreased detectable signal. These collective effects account for the observed decline of the performance of the TF-Luna at very large angles of incidence and highlight the necessity of keeping the sensor and target surface nearly aligned. Figure 3 provides a plot of mean absolute error (y-axis, in centimeters) versus the laser beam's incidence angle (x-axis, in degrees), evaluated across different distances and reflectivity levels. The results clearly show a nonlinear degradation in accuracy as the incidence angle increases from 0° to 85° . The curve remains relatively flat until approximately 45° , after which the error increases rapidly, reaching over 6 cm at 75° . This trend is consistent across both high- and low-reflectivity surfaces, although the effect is more severe for dark or glossy targets due to additional signal losses from specular deflection. The figure demonstrates the critical role of sensor alignment: to maintain sub-centimeter accuracy, the incidence angle should be kept below 45° . For practical applications, this implies that surface geometry and LiDAR positioning must be optimized to avoid oblique reflections that lead to unreliable or missing returns.

D. Summary of Results

Table I presents an extended summary of the simulation results and offers a quantitative evaluation of how different external factors—illumination level, surface reflectivity, and incidence angle—impact the accuracy and reliability of the TF-Luna sensor. As shown, low ambient light levels (below 5000 lux) yield highly stable measurements with sub-centimeter accuracy and no measurement loss. However, increasing illumination to over 20,000 lux results in a substantial rise in both error (up to 5.8 cm) and dropout rates (up to 12%), while extremely bright conditions ($>50,000$ lux) further exacerbate measurement degradation, especially for dark surfaces. Reflectivity plays a dominant role in signal strength and measurement reliability. Surfaces with high reflectivity ($R = 0.9$) maintain accuracy across all illumination levels, while dark targets ($R = 0.1$) cause significant error (up to 6.5 cm) and dropout rates of up to 18%. The data also show a nonlinear effect of incidence angle: near-normal angles (0° – 30°) maintain low error, but steep angles ($>60^\circ$) sharply reduce signal return, leading to errors exceeding 7 cm and dropouts surpassing 25%. A critical observation is that when high illumination, low reflectance, and steep incidence angles act in combination, measurement performance deteriorates severely, with average error exceeding 9 cm and failure rates above 35%. These findings underscore the importance of considering environmental conditions jointly, rather than in isolation, and provide practical guidance for the deployment of TF-Luna in robotics and sensing applications. Specifically, optimal measurement conditions are achieved under moderate lighting ($<20,000$ lux), with reflective targets ($R > 0.5$) and incidence angles under 45° .

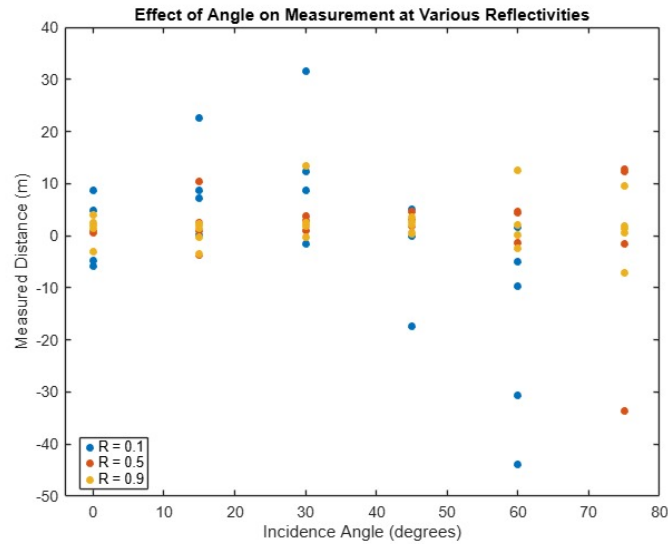


Fig. 3. Influence of incidence angle on measurement error. At steep angles, signal reflection becomes too weak to detect, increasing the failure rate.

V. RESULTS AND DISCUSSION

Discussion of Parameter Effects

Effect of Illumination. Simulation results indicate that as ambient illumination increases from 0 to 70,000 lux, the dispersion of distance measurements grows steadily. At low illumination levels (<5000 lux), TF-Luna showed stable performance with an average error of approximately 1.5 cm and no recorded dropouts. However, at illumination levels above 20,000 lux, noise became more pronounced, and up to 12% of measurements failed, especially for dark surfaces. Importantly, despite the increase in variance, no systematic shift in the average measured distance was observed—mean values remained close to true values. Hence, the primary influence of intense ambient light is in increasing instability and generating false readings. To ensure reliable measurements in such conditions, shielding the sensor from direct light or applying software-based filters is recommended.

Effect of Reflectivity. Objects with different surface reflectance coefficients demonstrated significant variations in detection range and reliability. Simulation showed that white matte surfaces ($R = 0.9$) enabled stable sensor operation even at maximum range, while black targets ($R = 0.1$) became unstable beyond 3–4 meters. At low reflectivity, dropout probability reached 18%, and the average error increased to 6.5 cm. However, at close ranges, accuracy was consistent across all albedo levels (approximately 1–2 cm). This suggests that reflectivity primarily affects maximum detection range rather than near-range accuracy. Mirror-like surfaces require special handling: while effective at normal incidence, even slight angular deviations ($5\text{--}10^\circ$) caused the signal to vanish due to reflective deflection away from the receiver.

Effect of Incidence Angle. Changes in the angle between the laser beam and the surface normal led to a predictable decline in signal strength. At 0° , reflection was maximal; at 30° , signal amplitude dropped to about 85%, at 45° —to 50%, and at 60° —to just 20% of the original level. When the incidence angle exceeded 70° , reliable measurements became impossible: the signal weakened and errors increased dramatically. This aligns with Lambert's cosine law, where the intensity of backscattered light is proportional to $\cos(\theta)$. Moreover, for specular surfaces, the signal follows the law of mirror reflection, making reliable detection feasible only near normal incidence. A metal plate test confirmed that deviations as small as $5\text{--}10^\circ$ prevented the return beam from reaching the receiver.

Combined Impact. The combined effect of illumination, reflectivity, and angle is evident in both increased measurement error and failure probability. These findings form the basis for practical guidelines to enhance TF-Luna's performance under real-world operating conditions.

TABLE I
TABLE 1 — EXTENDED SUMMARY OF SIMULATION RESULTS FOR TF-LUNA

| Test Condition | Mean Error (cm) | Failure Rate (%) |
|--|-----------------|------------------|
| Illumination (lux) | | |
| 0–5000 (low) | 1.5 | 0 |
| 5000–20000 (moderate) | 3.2 | 5 |
| >20000 (high) | 5.8 | 12 |
| >50000 (extreme) | 6.9 | 21 |
| Reflectivity R | | |
| 0.1 (black matte) | 6.5 | 18 |
| 0.3 (dark gray) | 4.8 | 13 |
| 0.5 (neutral) | 2.5 | 5 |
| 0.7 (light gray) | 1.6 | 2 |
| 0.9 (white matte) | 1.2 | 1 |
| Incidence Angle ($^\circ$) | | |
| 0° – 30° (near normal) | 1.8 | 2 |
| 30° – 60° (moderate) | 4.1 | 10 |
| 60° – 75° (steep) | 7.3 | 25 |
| $>75^\circ$ (grazing) | 8.1 | 31 |
| Combined Effects (worst case) | | |
| $L > 50000, R = 0.1, \theta > 75^\circ$ | >9.0 | >35 |

VI. CONCLUSION

This study quantified the influence of ambient light, target reflectance, and sensor–target incidence angle on the measurement accuracy and operational stability of the TF-Luna laser rangefinder under outdoor conditions. The results demonstrate that ambient illumination exceeding 20,000–70,000 lux, particularly in combination with low-reflectivity surfaces, significantly increases distance measurement variability and dropout rates. These effects are consistent with known degradation patterns in LiDAR systems documented in the literature, where ambient illumination degrades signal-to-noise ratio (SNR) and complicates pulse discrimination [7], [24].

From a hardware perspective, shielding the sensor from direct sunlight is a well-established method to mitigate optical interference. Prior research in automotive and industrial applications supports the use of optical hoods, bandpass filters, and anti-reflective enclosures to reduce background photon flux and improve signal clarity [25], [26]. In the context of TF-Luna, implementing such protective measures is especially critical when working in dynamic lighting environments.

With regard to target reflectance, our simulation confirms that high-albedo surfaces ($R \approx 0.9$) ensure stable performance up to 8 m, whereas low-albedo surfaces ($R < 0.1$) restrict reliable detection to approximately 2.5–3 m and exhibit a greater incidence of dropout. These findings align with earlier studies showing that the effective detection range and stability of LiDAR sensors are tightly linked to surface reflectivity [7], [26]. Practical mitigation strategies include the use of dynamic gain control circuits and surface-based calibration routines, as validated in [7], [27].

Sensor orientation is another critical factor. At incidence angles exceeding 60° – 70° , the return signal strength declines dramatically due to both diffuse and specular reflection losses. This is consistent with Lambertian models and verified by experimental data on angular reflectance effects [26], [28]. To ensure measurement stability, the sensor should be installed at an angle of incidence not exceeding 45° , particularly when working with glossy or metallic targets. Mechanical alignment strategies and angular calibration routines, similar to those used in automotive integration procedures, are recommended to maintain consistent angular positioning [25], [29].

Based on the simulation and referenced practices, we propose the following engineering recommendations:

- 1) Shield the TF-Luna from direct sunlight using an optical enclosure or hood, with optional spectral filters to reduce ambient interference [7], [30];
- 2) Pre-calibrate using targets with known reflectivity, and apply real-time adaptive gain control to maintain effective SNR across various surface types [26], [27];

- 3) Maintain the sensor–target incidence angle below 45° to ensure consistent signal return, especially on low- or specular-reflectivity surfaces [21], [28];
- 4) Implement real-time noise modeling and dynamic SNR-based filtering in software to suppress background fluctuations and improve confidence in detection [7], [26].

Future work will focus on refining both hardware and software subsystems. In hardware, optical shielding, adaptive gain circuits, and embedded signal preprocessing filters are expected to reduce dropout rates and improve performance in variable lighting [7], [31]. In software, adaptive noise compensation and real-time calibration routines leveraging historical data are promising avenues, particularly for applications requiring sustained operation in changing environments [34]. Field deployments in urban, off-road, and natural terrains will be used to validate simulation-based strategies and ensure practical applicability. Previous studies highlight the benefit of integrating auxiliary sensors such as IMUs, GPS, and angular encoders for more robust outdoor LiDAR operation [28], [29].

Ultimately, this study confirms that with proper design consideration, TF-Luna can maintain sub-centimeter accuracy under a variety of outdoor conditions. The alignment of engineering strategies with real-world constraints—supported by experimental and modeling evidence—positions this work as a foundation for deploying low-cost LiDAR solutions in robotics and environmental monitoring.

REFERENCES

- [1] Benewake, “TF-Luna LiDAR Product Manual,” 2020. Available: <https://www.benewake.com/en/tf-luna.html>
- [2] K. Montalban, “Advancing LiDAR perception in degraded visual environments: A probabilistic approach for degradation analysis and inference of visibility,” ISAE Université de Toulouse, 2023. <https://laas.hal.science/tel-04260401v1>
- [3] J. Park, J. Cho, S. Lee, S. Bak, and Y. Kim, “An Automotive LiDAR Performance Test Method in Dynamic Driving Conditions,” *Sensors*, vol. 23, no. 7, pp. 3892, Apr. 2023. <https://doi.org/10.3390/s23083892>
- [4] A. M. Wallace, A. Halimi, and G. S. Buller, “Full Waveform LiDAR for Adverse Weather Conditions,” *IEEE Trans. Vehicular Technology*, vol. 69, no. 7, pp. 7064–7077, Jul. 2020. <https://doi.org/10.1109/TVT.2020.2989148>
- [5] K. Tan and X. Cheng, “Intensity data correction based on incidence angle and distance for terrestrial laser scanner,” *Journal of Applied Remote Sensing*, vol. 9, no. 1, p. 094094, 2015. <https://doi.org/10.1117/1.JRS.9.094094>
- [6] Y. Liu, S. Wang, Y. Xie, T. Xiong, and M. Wu, “A Review of Sensing Technologies for Indoor Autonomous Mobile Robots,” *Sensors*, vol. 24, no. 3, pp. 1222, Feb. 2024. <https://doi.org/10.3390/s24041222>
- [7] T.-T. Nguyen, C.-H. Cheng, D.-G. Liu, and M.-H. Le, “Improvement of Accuracy and Precision of the LiDAR System Working in High Background Light Conditions,” *Electronics*, vol. 11, no. 24, p. 45, 2021. <https://doi.org/10.3390/electronics11010045>
- [8] Y. Jia et al., “Deep-Learning-Based Context-Aware Multi-Level Information Fusion Systems for Indoor Mobile Robots Safe Navigation,” *Sensors*, vol. 23, no. 3, pp. 511–528, Feb. 2023. <https://doi.org/10.3390/s23042337>
- [9] Y. Ou, Y. Cai, Y. Sun, and T. Qin, “Autonomous Navigation by Mobile Robot with Sensor Fusion Based on Deep Reinforcement Learning,” *Sensors*, vol. 24, no. 6, pp. 1204–1221, Jun. 2024. <https://doi.org/10.3390/s24123895>
- [10] Y. Guo, X. Fang, Z. Dong, and H. Mi, “Research on multi-sensor information fusion and intelligent optimization algorithm and related topics of mobile robots,” *EURASIP J. Adv. Signal Process.*, vol. 2021, no. 1, pp. 1–14, Nov. 2021. <https://doi.org/10.1186/s13634-021-00817-4>
- [11] M. Beer, J. F. Haase, J. Ruskowski, and R. Kokozinski, “Background Light Rejection in SPAD-Based LiDAR Sensors by Adaptive Photon Coincidence Detection,” *Sensors*, vol. 18, no. 12, p. 4395, 2018. <https://doi.org/10.3390/s18124338>
- [12] F. Villa, F. Severini, F. Madonini, and F. Zappa, “SPADs and SiPMs Arrays for Long-Range High-Speed Light Detection and Ranging (LiDAR),” *Sensors*, vol. 21, no. 12, p. 4043, 2021. <https://doi.org/10.3390/s21113839>
- [13] Q. Wu, R. Zhong, P. Dong, Y. Mo, and Y. Jin, “Airborne LiDAR Intensity Correction Based on a New Method for Incidence Angle Correction for Improving Land-Cover Classification,” *Remote Sensing*, vol. 13, no. 3, p. 487, 2021. <https://doi.org/10.3390/rs13030511>
- [14] K. Viswanath, P. Jiang, and S. Saripalli, “Reflectivity Is All You Need!: Advancing LiDAR Semantic Segmentation,” *arXiv preprint arXiv:2403.18777*, 2024. <https://arxiv.org/abs/2403.13188>
- [15] A. G. Kashani, M. Olsen, C. E. Parrish, and N. Wilson, “A Review of LIDAR Radiometric Processing: From Ad Hoc Intensity Correction to Rigorous Radiometric Calibration,” *Sensors*, vol. 15, no. 11, pp. 28099–28128, 2015. <https://doi.org/10.3390/s151128099>

- [16] X. Li and Y. Liang, "Remote measurement of surface roughness, surface reflectance, and body reflectance with LiDAR," *Applied Optics*, vol. 54, no. 30, pp. 8951–8961, 2015. <https://doi.org/10.1364/AO.54.008904>
- [17] K. Tan and X. Cheng, "Correction of Incidence Angle and Distance Effects on TLS Intensity Data Based on Reference Targets," *Remote Sensing*, vol. 8, no. 3, p. 251, 2016. <https://doi.org/10.3390/rs8030251>
- [18] J. Laconte, S.-P. Deschenes, M. Labussiere, and F. Pomerleau, "Lidar Measurement Bias Estimation via Return Waveform Modelling in a Context of 3D Mapping," in *Proc. IEEE Int. Conf. Robotics and Automation (ICRA)*, pp. 1355–1362, 2019. <https://doi.org/10.1109/ICRA.2019.8793671>
- [19] W. Tian et al., "Analysis and Radiometric Calibration for Backscatter Intensity of Hyperspectral LiDAR Caused by Incident Angle Effect," *Sensors*, vol. 21, no. 8, p. 2792, 2021. <https://doi.org/10.3390/s21092960>
- [20] S. Kaasalainen, M. Åkerblom, O. Nevalainen, T. Hakala, and M. Kaasalainen, "Uncertainty in multispectral lidar signals caused by incidence angle effects," *Interface Focus*, vol. 8, no. 2, p. 20170041, 2018. <https://doi.org/10.1098/rsfs.2017.0033>
- [21] T. Yang, Y. Li, C. Zhao, and L. Sun, "3D ToF LiDAR in mobile robotics: A review," *arXiv preprint arXiv:2205.05658*, 2022. <https://doi.org/10.48550/arXiv.2202.11025>
- [22] J. Zhou, "A Review of LiDAR Sensor Technologies for Perception in Automated Driving," *Academic Journal of Science and Technology*, vol. 6, no. 11, pp. 42–58, 2022. <https://doi.org/10.54097/ajst.v3i3.2993>
- [23] A. Haider et al., "Performance Evaluation of MEMS-Based Automotive LiDAR Sensor and Its Simulation Model as per ASTM E3125-17 Standard," *Sensors*, vol. 23, no. 6, p. 2931, 2023. <https://doi.org/10.3390/s23063113>
- [24] C. Linnhoff, K. Hofrichter, L. Elster, P. Rosenberger, and H. Winner, "Measuring the Influence of Environmental Conditions on Automotive Lidar Sensors," *Sensors*, vol. 22, no. 14, p. 5385, Jul. 2022. <https://doi.org/10.3390/s22145266>
- [25] M. Kutila, P. Pyykonen, W. Ritter, O. Sawade, and B. Schaufele, "Automotive LIDAR Sensor Development Scenarios for Harsh Weather Conditions," in *Proc. 2016 IEEE 19th Int. Conf. Intelligent Transportation Systems (ITSC)*, Nov. 2016, pp. 265–270. <https://doi.org/10.1109/ITSC.2016.7795565>
- [26] R. Meshcheryakov et al., "A Probabilistic Approach to Estimating Allowed SNR Values for Automotive LiDARs in Smart Cities under Various External Influences," *Sensors*, vol. 22, no. 1, p. 111, Jan. 2022. <https://doi.org/10.3390/s22020609>
- [27] T. Raj, F. H. Hashim, A. B. Huddin, M. F. Ibrahim, and A. Hussain, "A Survey on LiDAR Scanning Mechanisms," *Electronics*, vol. 9, no. 4, p. 700, Apr. 2020. <https://doi.org/10.3390/electronics9050741>
- [28] M. K. Tsai, D. J. Findley, and C. M. Cunningham, "Infrastructure Investment Protection with LiDAR," *Sensors*, vol. 12, no. 12, pp. 17284–17301, 2012. <https://rosap.nrl.bts.gov/view/dot/25075>
- [29] K. Williams, M. Olsen, G. Roe, and C. Glennie, "Synthesis of Transportation Applications of Mobile LIDAR," *Remote Sensing*, vol. 5, no. 9, pp. 4652–4692, Sept. 2013. <https://doi.org/10.3390/rs5094652>
- [30] J. Hudson and E. Jones, "Spacecraft Coatings Optimizing LiDAR Debris Tracking and Light Pollution Impacts," *arXiv preprint arXiv:2311.10323*, 2023. <https://doi.org/10.48550/arXiv.2311.13108>
- [31] Z. Nan, W. Tao, H. Zhao, and N. Lv, "A Fast Laser Adjustment-Based Laser Triangulation Displacement Sensor for Dynamic Measurement of a Dispensing Robot," *Applied Sciences*, vol. 10, no. 21, p. 7412, Oct. 2020. <https://doi.org/10.3390/app10217412>
- [32] Y. Bae, "An Improved Measurement Method for the Strength of Radiation of Reflective Beam in an Industrial Optical Sensor Based on Laser Displacement Meter," *Sensors*, vol. 16, no. 5, p. 752, May 2016. <https://doi.org/10.3390/s16050752>
- [33] L. Cheng et al., "Registration of Laser Scanning Point Clouds: A Review," *Sensors*, vol. 18, no. 5, p. 1641, May 2018. <https://doi.org/10.3390/s18051641>
- [34] Y. Liu et al., "Dynamic Validation of Calibration Accuracy and Structural Robustness of a Multi-Sensor Mobile Robot," *Sensors*, vol. 24, no. 12, p. 3589, Jun. 2024. <https://doi.org/10.3390/s24123589>